

## ELECTRO-RHEOLOGICALLY BASED CONTROL SYSTEM OF A COILING FUNCTION FOR A TENTACLE ARM

Mircea IVANESCU, Mihaela Cecilia FLORESCU

*Mechatronics Department, Faculty of Automation, Computers and Electronics,  
University of Craiova*

*ivanescu@robotics.ucv.ro, mihaelaflorescu@yahoo.com*

**Abstract** – The paper focuses on the control problem of a tentacle robot that performs the coil function of the grasping. First, the dynamic model of a tentacle arm with continuum elements produced by flexible composite materials in conjunction with active-controllable electro-rheological fluids is analyzed. Secondly, both problems, i.e. the position control and the force control are approached. The difficulties determined by the complexity of the non-linear integral-differential equations are avoided by using a very basic energy relationship of this system. Energy-based control laws are introduced for the position control problem. A force control method is proposed, namely the DSMC method in which the evolution of the system on the switching line by the ER fluid viscosity is controlled. Numerical simulation is also presented.

**Keywords:** *distributed parameter systems, grasping, tentacle robots, and force control.*

### 1. INTRODUCTION

A tentacle robot is a hyper-degree-of-freedom (HDOF) manipulator and there has been a rapidly expanding interest in its study and construction lately. The control of these systems is very complex. In [1], the control by cables or tendons designed to transmit forces to the elements of the arm in order to closely approximate the arm as a truly continuous backbone was analyzed. Gravagne [2] analyzed the kinematical model of “hyper-redundant” robots, known as “continuum” robots. Important results were obtained by Chirikjian and Burdick [3-6] which laid the foundations for the kinematical theory of hyper-redundant robots. Mochiyama has also investigated the problem of controlling the shape of an HDOF rigid-link robot with two-degree-of-freedom joints using spatial curves [7,8]. In [9, 10], the “state of art” of continuum robots are presented. In other papers [11, 12], several technological solutions for actuators used in hyper-redundant structures are presented and conventional control systems are introduced. Another paper [13] proposes a dynamic model for hyper-redundant structures such as an infinite degree-of-freedom continuum model and some computed torque control systems are introduced. In [14], a dynamic model for

an ideal planar tentacle system is presented and optimal control solutions are discussed. The difficulty of the dynamic control lies in the determined by integral-partial-differential models with high nonlinearities that characterize the dynamics of these systems. In [15], the dynamic model for 3D space is inferred and a control law based on the energy of the system is analyzed.

In this paper, the problem of a class of tentacle arms with continuum elements that performs the grasping function by coiling is discussed. First, the dynamic model of the system is inferred. The difficulties determined by the complexity of the non-linear integral-differential equations, which represent the dynamic model of the system, are avoided by using a basic energy relationship of this system. Energy-based control laws are introduced for the position control problem. A force control method is proposed, namely the DSMC (Direct Sliding Mode Control) method, the evolution of the system on the switching line by ER fluid viscosity control.

### 2. BACKGROUND

#### 2.1. Technological model

The paper studies a class of tentacle arms that can achieve any position and orientation in 3D space, and that can perform a coil function for the grasping (Figure 1).

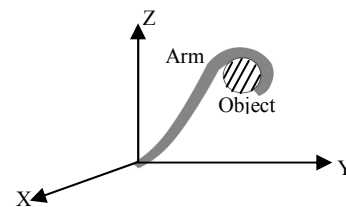


Figure 1. The tentacle grasping arm

Technologically, these arms are based on the use of flexible composite materials in conjunction with active controllable electro-rheological (ER) fluids that can change their mechanical characteristics in the presence of electrical fields. The general form of the arm is shown in Figure 2. It consists of a number (N) of

elements, cylinders made of fiber-reinforced rubber. There are four internal chambers in the cylinder, each of them containing the ER fluid with an individual control circuit. The last  $m$  elements ( $m < N$ ) represent the grasping terminal. These elements contain a number of force sensors distributed on the surface of the cylinders. These sensors measure the contact with the load and ensure the distributed force control during the grasping. The sensor network is constituted by a number of impedance devices (see Figure 3) that define the dynamic relationship between the grasping element displacement and the contact force.

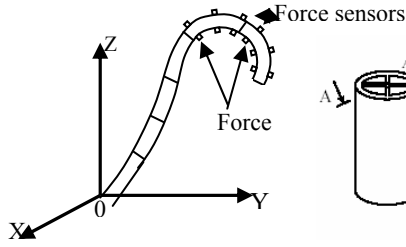


Figure 2. The force sensors distribution

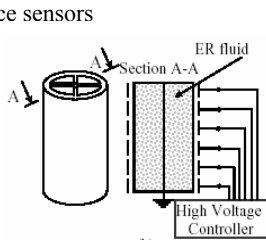


Figure 3. The cylinder structure

## 2.2. Theoretical model

The essence of the tentacle model is a 3-dimensional backbone curve  $C$  that is parametrically described by a vector  $r(s) \in R^3$  and an associated frame  $\phi(s) \in R^{3 \times 3}$  whose columns create the frame bases (Figure 4). The independent parameter  $s$  is related to the arc-length from the origin of the curve  $C$ ,  $s \in [0, L]$ , where:

$$L = \sum_{i=1}^N l_i \quad (1)$$

where  $l_i$  represent the length of the elements  $i$  of the arm in the initial position.

The position of a point  $s$  on curve  $C$  is defined by the position vector:

$$\bar{r} = \bar{r}(s), \quad s \in [0, l] \quad (2)$$

For a dynamic motion, the time variable will be introduced,  $\bar{r} = \bar{r}(s, t)$ . We used a parameterization of the curve  $C$  based upon two “continuous angles”  $\theta(s)$  and  $q(s)$  [3-6] and the length variable  $u$  (Figure 4). At each point  $\bar{r}(s, t)$ , the robot’s orientation is given by a right-handed orthonormal basis vector  $\{\bar{e}_x, \bar{e}_y, \bar{e}_z\}$  and its origin coincides with point  $\bar{r} = \bar{r}(s, t)$ . The position vector on curve  $C$  is given by:

$$\bar{r}(s, t) = [x(s, t) \quad y(s, t) \quad z(s, t)]^T \quad (3)$$

where the three parameters that appear in the relation

$$(3) \text{ are as follows: } x(s, t) = \int_0^s \sin \theta(s', t) \cos q(s', t) ds',$$

$$y(s, t) = \int_0^s \cos \theta(s', t) \cos q(s', t) ds', \quad z(s, t) = \int_0^s \sin q(s', t) ds',$$

with  $s' \in [0, s]$ .

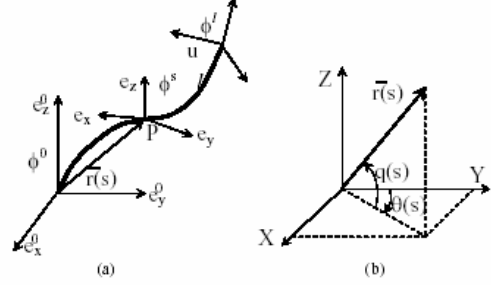


Figure 4. (a) The backbone structure; (b) The backbone parameters

We can adopt the following interpretation [2, 6]: at any point  $s$ , the parameters  $x(s, t)$ ,  $y(s, t)$  and  $z(s, t)$  determine the current position and  $\phi(s)$  determines the robot’s orientation. The robot’s shape is defined by the behaviour of functions  $\theta(s)$  and  $q(s)$ . The robot “grows” from the origin by integrating to get  $\bar{r}(s, t)$ ,  $s \in [0, l]$ . The velocity components are obtained by deriving the corresponding parameter of the robot movement [16]. For an element  $dm$ , where  $dm = \rho \cdot ds$ , the kinetic and gravitational potential energy will be:

$$dT = \frac{1}{2} dm (v_x^2 + v_y^2 + v_z^2 + v_u^2) \quad (7)$$

$$dV = dm \cdot g \cdot z \quad (8)$$

From (7) and (8), we obtain:

$$T = \frac{1}{2} \rho \int_0^l \left( \left( \int_0^s (-\dot{q}' \sin q' \sin \theta' + \dot{\theta}' \cos q' \cos \theta') ds' \right)^2 + \left( \int_0^s (-\dot{q}' \sin q' \cos \theta' - \dot{\theta}' \cos q' \cos \theta') ds' \right)^2 + \left( \int_0^s \dot{q}' \cos q' ds' \right)^2 \right) ds + \frac{1}{2} \rho \int_0^l \dot{u}^2 ds \quad (9)$$

$$V = \rho g \int_0^l \int_0^s \sin q' ds' ds \quad (10)$$

The elastic potential energy will be approximated by the bending of the element [10]:

$$V_{eb} = k \frac{d^2}{4} \sum_{i=1}^N (q_i^2 + \theta_i^2) \quad (11)$$

We assumed that each element has a constant curvature and a uniform equivalent elasticity coefficient  $k$  (constant on all the length of the arm). We shall consider  $F_\theta(s, t)$ ,  $F_q(s, t)$  the distributed forces on the arm length that determine motion and orientation in the  $\theta$ - and  $q$ -plane. From [14], the mechanical work is:

$$L = \int_0^l \int_0^t (F_\theta(s, \tau) \dot{\theta}(s, \tau) + F_q(s, \tau) \dot{q}(s, \tau)) d\tau ds \quad (12)$$

where  $\dot{\theta}(s, t) = \frac{\partial \theta}{\partial t}(s, t)$  and  $\dot{q}(s, t) = \frac{\partial q}{\partial t}(s, t)$ .

The energy-work relationship will be

$$\begin{aligned} & [T(t) + V(t)] - [T(0) + V(0)] = \\ & = \int_0^l \int_0^t (F_\theta(s, \tau) \dot{\theta}(s, \tau) + F_q(s, \tau) \dot{q}(s, \tau)) d\tau ds \end{aligned} \quad (13)$$

where  $T(t)$ ,  $T(0)$  and  $V(t)$ ,  $V(0)$  are the total kinetic energy and total potential energy of the system at the time  $t$  and 0, respectively.

### 3. DYNAMIC MODEL

The robot model is considered a distributed parameter system defined on a variable spatial domain  $\Omega = [0, L]$  and the spatial coordinate  $s$ . The dynamic model is derived by using Lagrange equations:

$$\frac{\partial}{\partial t} \left( \frac{\delta T}{\delta \dot{\theta}(t, s)} \right) - \frac{\delta T}{\delta \theta(t, s)} + \frac{\delta V}{\delta \theta(t, s)} + \frac{\delta V_e}{\delta \theta(t, s)} = F_\theta \quad (14)$$

$$\frac{\partial}{\partial t} \left( \frac{\delta T}{\delta \dot{q}(t, s)} \right) - \frac{\delta T}{\delta q(t, s)} + \frac{\delta V}{\delta q(t, s)} + \frac{\delta V_e}{\delta q(t, s)} = F_q \quad (15)$$

where  $\partial/\partial(\cdot)$ ,  $\delta/\delta(\cdot)$  denote the classical and functional partial derivatives. From (9), (10), (11), the distributed parameter model becomes,

$$\begin{aligned} & \rho \int_0^s \int_0^s (\ddot{q}' (\sin q' \sin q'' \cos(q' - q'') + \cos q' \cos q'') - \\ & - \ddot{\theta}' \cos q' \sin q'' \sin(\theta'' - \theta') + \\ & + (\dot{q}')^2 (\cos q' \sin q'' \cos(\theta' - \theta'') - \sin q' \cos q'') + \\ & + (\dot{\theta}')^2 \cos q' \sin q'' \cos(\theta' - \theta'') - \\ & - \dot{q}' \dot{q}'' \sin(q'' - q')) ds' ds'' + \rho g \int_0^s \cos q' ds' = F_q \end{aligned} \quad (16)$$

$$\begin{aligned} & \rho \int_0^s \int_0^s (\ddot{q}' \sin q' \cos q'' \sin(\theta'' - \theta') + \\ & + \ddot{\theta}' \cos q' \cos q'' \cos(\theta'' - \theta') - \\ & - (\dot{q}')^2 \cos q' \cos q'' \sin(\theta'' - \theta') + \\ & + (\dot{\theta}')^2 \cos q' \cos q'' \sin(\theta'' - \theta') - \\ & - \dot{\theta}' \dot{q}' \sin q' \cos q'' \cos(\theta'' - \theta')) ds' ds'' = F_\theta \end{aligned} \quad (17)$$

where we used the notations:  $\dot{q}' = \partial q(s', t) / \partial t$ ,  $\ddot{q}' = \partial^2 q(s', t) / \partial t^2$ ,  $F_q = F_q(s, t)$ ,  $s \in [0, L]$ ,  $s' \in [0, s]$ .

The state of this system at any fixed time  $t$  is specified by the set  $(\omega(t, s), \nu(t, s))$ , where  $\omega = [\theta \ q]^T$  represents the generalized coordinates and  $\nu$  defines the momentum densities. The set of all functions  $s \in \Omega$  that  $\omega$ ,  $\nu$  can take on at any time is the state function space  $\Gamma(\Omega)$ . We shall assume that  $\Gamma(\Omega) \subset L_2(\Omega)$ .

The control forces have the distributed components along the arm,  $F_\theta(s, t)$ ,  $F_q(s, t)$ ,  $s \in [0, L]$  that are determined by the lumped torques,

$$F_\theta(s, t) = \sum_{i=1}^N \delta(s - il) \tau_{\theta_i}(t) \quad (18)$$

$$F_q(s, t) = \sum_{i=1}^N \delta(s - il) \tau_{q_i}(t) \quad (19)$$

where  $\delta$  is Kronecker delta,  $l_1 = l_2 = \dots = l_N = l$ , and

$$\tau_{\theta_i}(t) = (p_{\theta_i}^1 - p_{\theta_i}^2) S \cdot d/8 \quad (20)$$

$$\tau_{q_i}(t) = (p_{q_i}^1 - p_{q_i}^2) S \cdot d/8, \quad i = 1, 2, \dots, N \quad (21)$$

In (20), (21),  $p_{\theta_i}^1$ ,  $p_{\theta_i}^2$ ,  $p_{q_i}^1$ ,  $p_{q_i}^2$  represent the fluid pressure in the two chamber pairs,  $\theta$ ,  $q$  and  $S$ ,  $d$  are section area and the diameter of the cylinder, respectively (Figure 5).

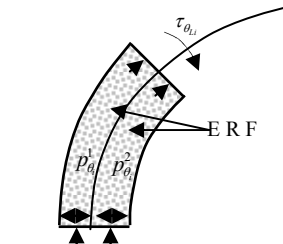


Figure 5. The cylinder driving

The pressure control of the chambers is described by the equations:

$$a_{ki}(\theta) \frac{dp_{\theta}^k}{dt} = u_{\theta ki} \quad (22)$$

$$b_{ki}(q) \frac{dp_{qi}^k}{dt} = u_{qi ki}, \quad k=1,2; \quad i=1,2,\dots,N \quad (23)$$

where  $a_{ki}$ ,  $b_{ki}$  are the coefficients determined by the fluid parameters and the geometry of the chambers and  $a_{ki}(0) > 0$ ,  $b_{ki}(0) > 0$ ,  $\theta, q \in \Gamma(\Omega)$ .

#### 4. CONTROL PROBLEM

The tentacle arm control problem of a grasping function by coiling is generated from two subproblems: the position control of the arm around the object-load and the force control of grasping.

##### 4.1. Position control

We consider that the initial state of the system is given by

$$\omega_0 = \omega(0, s) = [\theta_0, \quad q_0]^T \quad (24)$$

$$\nu_0 = \nu(0, s) = [0, \quad 0]^T \quad (25)$$

where  $\theta_0 = \theta(0, s)$ ,  $q_0 = q(0, s)$ ,  $s \in [0, L]$ , corresponding to the initial position of the arm defined by the curve  $C_0$

$$C_0 : (\theta_0(s), \quad q_0(s)), \quad s \in [0, L] \quad (26)$$

The desired point in  $\Gamma(\Omega)$  is represent by a desired position of the arm, the curve  $C_d$  that coils the load,

$$\omega_d = [\theta_d, \quad q_d]^T, \quad \nu_d = [0, \quad 0]^T \quad (27)$$

$$C_d : (\theta_d(s), \quad q_d(s)), \quad s \in [0, L] \quad (28)$$

In a grasping function by coiling, only the last  $m$  elements ( $m < N$ ) are used. Let  $l_g$  be the active grasping length,

$$l_g = \sum_{i=m}^n l_i \quad (29)$$

Let  $C_b$  be the curve defines the boundary of the load and we denote by  $O_b$  the origin of the coiling function, when  $O_b$  is the intersection between the tangent from origin  $O$  and the curve  $C_L$  (Figure 6.b).

This curve can be expressed using the coordinates  $(\theta, q) \in \Gamma(\Omega)$ .

$$C_b : (\theta_b(s^*), \quad q_b(s^*)), \quad s^* \in [0, L_b] \quad (30)$$

where  $L_b$  is the length of the coiling measured on the boundary  $C_b$  and  $s = L - l_g + s^*$ .

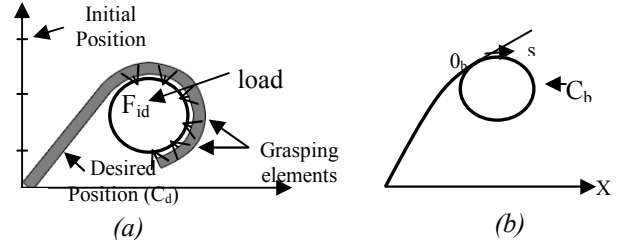


Figure 6. (a) The grasping position; (b) The grasping parameters

We define the position error by  $e_p(t)$

$$e_p(t) = \int_{L-l_g}^L ((\theta(s, t) - \theta_b(s)) + (q(s, t) - q_b(s))) ds \quad (31)$$

It is difficult to measure practically the angles  $\theta$ ,  $q$  for all  $s \in [0, L]$ . These angles can be evaluated or measured at the terminal point of each element. In this case, the relation (31) becomes

$$e_p(t) = \sum_{i=m}^N ((\theta_i(t) - \theta_{bi}) + (q_i(t) - q_{bi})) \quad (32)$$

The error can also be expressed with respect to the global desired position  $C_d$

$$e_p(t) = \sum_{i=1}^N ((\theta_i(t) - \theta_{di}) + (q_i(t) - q_{di})) \quad (33)$$

$$e_p(t) = \sum_{i=1}^N (e_{\theta_i}(t) + e_{q_i}(t)) \quad (34)$$

The position control of the arm means the motion control from the initial position  $C_0$  to the desired position  $C_b$  in order to minimize the error.

**Theorem 1.** The closed-loop control system of the position (16), (17), (22), (23) is stable if the fluid pressure control laws in the chambers of the elements are given by:

$$u_{\theta i}(t) = -a_{ji}(\theta) (k_{\theta}^{j1} \dot{e}_{\theta}(t) + k_{\theta}^{j2} \ddot{e}_{\theta}(t)) \quad (35)$$

$$u_{q i}(t) = -b_{ji}(\theta) (k_{q i}^{j1} \dot{e}_{q i}(t) + k_{q i}^{j2} \ddot{e}_{q i}(t)), \quad (36)$$

where  $j=1,2; i=1,2,\dots,N$ , with initial conditions:

$$p_{\theta}^1(0) - p_{\theta}^2(0) = (k_{\theta}^{11} - k_{\theta}^{21}) e_{\theta}(0) \quad (37)$$

$$p_{q i}^1(0) - p_{q i}^2(0) = (k_{q i}^{11} - k_{q i}^{21}) e_{q i}(0) \quad (38)$$

$$\dot{e}_{\theta_i}(0) = 0, \dot{e}_{q_i}(0) = 0 \quad (39)$$

and the coefficients  $k_{\theta_i}$ ,  $k_{q_i}$ ,  $k_{\theta_i}^{mn}$ ,  $k_{q_i}^{mn}$  are positive and verify the conditions

$$k_{\theta_i} = \frac{Sd}{8}(k_{\theta_i}^{11} - k_{\theta_i}^{21}), k_{q_i} = \frac{Sd}{8}(k_{q_i}^{11} - k_{q_i}^{21}) \quad (40)$$

$$k_{\theta_i}^{11} > k_{\theta_i}^{21}; k_{\theta_i}^{12} > k_{\theta_i}^{22}; k_{q_i}^{11} > k_{q_i}^{21}; k_{q_i}^{12} > k_{q_i}^{22} \quad (41)$$

## 4.2. Force control

The grasping by coiling of the continuum terminal elements offers a very good solution to remove the uncertainty connected to the geometry of the contact surface. The contact between an element and the load is presented in Figure 7. It is assumed that the grasping is determined by the chambers in the  $\theta$ -plane.

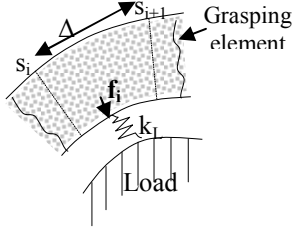


Figure 7. The grasping force

The relation between the fluid pressure and the grasping forces can be inferred for a steady state as:

$$\int_0^l k \frac{\partial^2 \theta(s)}{\partial s^2} ds + \int_0^l f(s) \tilde{T} \tilde{\theta}(s) ds = (p_1 - p_2) S \frac{d}{8} \quad (42)$$

where

$$\tilde{T} = \begin{bmatrix} 0 & 1 \\ -1 & 0 \end{bmatrix}; \tilde{\theta}(s) = \begin{bmatrix} \cos \theta \\ \sin \theta \end{bmatrix} \quad (43)$$

and  $f(s)$  is the orthogonal force on the curve  $C_b$ ,  $f(s)$  is  $F_\theta(s)$  in  $\theta$ -plane and  $F_q(s)$  in  $q$ -plane, respectively.

A spatial discretization  $s_1, s_2, \dots, s_{l_1}$  is introduced and  $\Delta = s_{i+1} - s_i$ , with  $\theta_i = \theta(s_i)$  and  $i = 1, 2, \dots, l_1$ . For small variation  $\Delta\theta_i$  around the desired position  $\theta_{id}$ , in  $\theta$ -plane, the dynamic model (16) can be approximated by the following discrete model [12]:

$$m_i \Delta \ddot{\theta}_i + c_i \Delta \dot{\theta}_i + H_i(\theta_{id} + \Delta\theta_i, \theta_{id}, q_d) - H(\theta_{id}, q_d) = d_i (f_i - F_{ei}) \quad (44)$$

where  $m_i = \rho S \Delta$ ,  $i = 1, 2, \dots, l_1$ ,  $H(\theta_{id}, q_d)$  is a nonlinear function defined on the desired position  $(\theta_{id}, q_d)$ ,  $c_i = c_i(v, \theta_i, q_d) > 0$ ,  $\theta, q \in \Gamma(\Omega)$ , with  $v$  - the viscosity of the fluid in the chambers.

$$H_i(\theta_{id} + \Delta\theta_i, \theta_{id}, q_d) - H(\theta_{id}, q_d) \cong \frac{\partial H_i}{\partial \theta} \Big|_{\theta=\theta_{id}, q=q_d} \Delta\theta_i = h_i(\theta_{id}, q_d) \cdot \Delta\theta_i \quad (45)$$

$F_{ei}$  is the external force due to the load.

The equation (44) becomes,

$$m_i \Delta \ddot{\theta}_i + c_i(v, \theta_i, q_d) \Delta \dot{\theta}_i + h_i(\theta_{id}, q_d) \cdot \Delta\theta_i = d_i (f_i - F_{ei}) \quad (46)$$

The aim of the explicit force control is to exert a desired force  $F_{id}$ . If the contact with the load is modeled as a linear spring with constant stiffness  $k_L$ , the environment force can be modeled as:

$$F_{ei} = k_L \Delta\theta_i \quad (47)$$

The error of the force control may be introduced in the form of

$$e_{fi} = F_{ie} - F_{id} \quad (48)$$

It may be easily shown that the equation (46) becomes

$$\frac{m_i}{k_L} \ddot{e}_{fi} + \frac{c_i}{k_L} \dot{e}_{fi} + \left( \frac{h_i}{k} + d_i \right) e_{fi} = d_i f_i - \left( \frac{h_i}{k} + d_i \right) F_{id} \quad (49)$$

**Theorem 2.** The closed force control system is asymptotic stable if the control law is

$$f_i = \frac{1}{k_L d_i} \left( (h_i + k_L d_i + m_i \sigma^2) e_{fi} - (h_i - k_L d_i) F_{id} \right) \quad (50)$$

$$c_i > m_i \sigma \quad (51)$$

In this paper, the force error control may be improved by using the Direct Sliding Mode Control [12].

**Proposition.** The DSMC control is ensured if the coefficients  $c_i$  of the control system verify the conditions:

$$c_i^2 > 4m_i (h_i + d_i k_L) \quad (52)$$

The condition (52) can be verified by increasing the viscosity of ER fluid. The force control system is developed into two steps. In the first step, according to Theorem 2, the trajectory of the error is controlled by the force  $f_i$ . In the second step, the viscosity of the fluid is increased and the trajectory switches directly toward the origin on the switching line. The block scheme of the force control is presented in Figure 8.

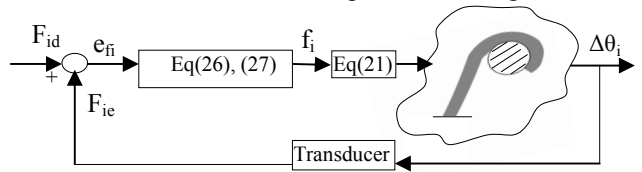


Figure 8. The force control system

## 5. SIMULATION

A hyperredundant manipulator with eight elements is considered. The mechanical parameters are: linear density  $\rho = 2.2 \text{ kg/m}$  and the length of one element is  $l = 0.05 \text{ m}$ . The initial position is the defined by

$$C_0 : \left( \theta_0(s) = \frac{\pi}{2} \right).$$

A discretisation for each element with an increment  $\Delta = l/3$  is introduced.

A force control for the grasping terminals is simulated. The phase portrait of the force error is presented in Figure 9. First, the control (26), (27) is used and then, when the trajectory penetrates the switching line the viscosity is increased for a damping coefficient  $\xi = 1.15$ .

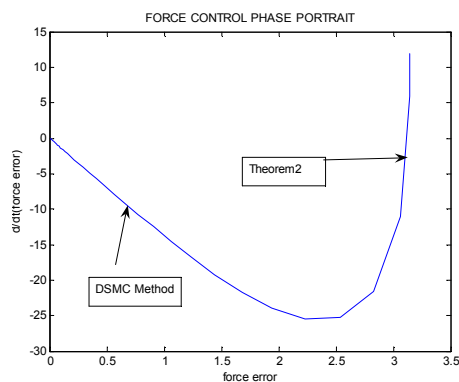


Figure 9. The force control phase portrait

## 6. CONCLUSION

The paper treats the control problem of a tentacle robot arm with continuum elements that performs the coil function of grasping. The structure of the arm is given by flexible composite materials in conjunction with active-controllable electro-rheological fluids. The dynamic model of the system is inferred by using Lagrange equations developed for infinite dimensional systems.

The grasping problem comprises in two subproblems: the position control and the force control. The difficulties determined by the complexity of the non-linear integral-differential equations are avoided by using a very basic energy relationship of this system and energy-based control laws are introduced for the position control problem. The force control is obtained by using the DSMC method in which the evolution of the system on the switching line is controlled by the ER fluid viscosity. Numerical simulation is presented.

## References

- [1] A. Hemami, *Design of light weight flexible robot arm*, Robots 8 Conference Proceedings, Detroit, USA, June 1984, pp. 1623-1640.
- [2] Ian A. Gravagne, Ian D. Walker, *On the kinematics of remotely - actuated continuum robots*, Proc. 2000 IEEE Int. Conf. on Rob. and Aut., San Francisco, April 2000, pp. 2544-2550.
- [3] G. S. Chirikjian, J. W. Burdick, *An obstacle avoidance algorithm for hyper-redundant manipulators*, Proc. IEEE Int. Conf. on Rob. and Aut., Cincinnati, Ohio, May 1990, pp. 625 - 631.
- [4] G.S. Chirikjian, J. W. Burdick *Kinematically optimal hyperredundant manipulator configurations*, Proc. IEEE Int. Conf. on Robotics and Automation, Nice, May 1992, pp. 415 - 420.
- [5] G.S. Chirikjian, *A general numerical method for hyper-redundant manipulator inverse kinematics*, Proc. IEEE Int. Conf. on Robotics and Automation, Atlanta, May 1993, pp. 107 - 112.
- [6] G.S. Chirikjian, J. W. Burdick *Kinematically optimal hyperredundant manipulator configurations*, IEEE Trans. Robotics and Aut., vol. 11, no. 6, Dec. 1995, pp. 794 - 798.
- [7] H. Mochiyama, H. Kobayashi, *The shape Jacobian of a manipulator with hyper degrees of freedom*, Proc. 1999 IEEE Int. Conf. on Robotics and Aut., Detroit, May 1999, pp. 2837- 2842.
- [8] H. Mochiyama, E. Shimeura, H. Kobayashi, *Direct kinematics of manipulators with hyper degrees of freedom and Serret-Frenet formula*, Proc. 1998 IEEE Int. Conf. on Robotics and Aut., Leuven, Belgium, May 1998, pp. 1653-1658.
- [9] G. Robinson, J.B.C. Davies, *Continuum robots – a state of the art*, IEEE Int.Conf.on Rob. and Aut., Detroit, Michigan, May 1999, pp. 2849-2854.
- [10] K. Suzumori, S. Iikura, H. Tanaka, *Development of flexible microactuator and its application to robot mechanisms*, IEEE Conf. on Robotics and Aut., Sacramento CA, April 1991, pp 1564 - 1573.
- [11] S.K. Singh, D.O. Popa, *An Analysis and Some Fundamental Problems in Adaptive Control of Force*, IEEE Trans on Robotics and Aut., Vol 11 No 6, pp 912-922, 1993
- [12] M. Ivanescu, V. Stoian, *A variable structure controller for a tentacle manipulator*, IEEE Int. Conf. on Rob. and Aut., Nagoya 1995, pp. 3155-3160.
- [13] S. Chiaverini, B. Siciliano, L. Villani, *Force and Position Tracking: Parallel Control with Stiffness Adaptation*, IEEE Control Systems, Vol. 18 No 1, pp. 27-33, 1990
- [14] S.S. Ge, T.H. Lee, G. Zhu., *Energy-Based Robust Controller Design for Multi-Link Flexible Robots*, Mechatronics, No 7, Vol. 6, pp. 779-798, 1996
- [15] M. Ivanescu, *Position dynamic control for a tentacle manipulator*, IEEE Int. Conf. on Rob. and Aut., Washington, May 2002, pp. 1531-1539.